ACTA ACUSTICA UNITED WITH ACUSTICA
Vol. 95 (2009) 76 – 85
DOI 10.3813/AAA.918129

A Model to Predict the Sound Reflection from Forests

J. M. Wunderli
Empa, Swiss Federal Laboratories for Material Testing and Research, 8600 Duebendorf, Switzerland.
Jean-marc.wunderli@empa.ch

E. M. Salomons
TNO Science and Industry, 2628CK Delft, The Netherlands

Summary
A model is presented to predict the reflection of sound at forest edges. A single tree is modelled as a vertical cylinder. For the reflection at a cylinder an analytical solution is given based on the theory of scattering of spherical waves. The entire forest is represented by a line of cylinders placed along the forest edge. The spacing between the cylinders is defined as a function of frequency and geometrical properties to account for contributions from the depth of the forest. As a consequence of this model assumption of a single line of reflecting cylinders, a variable segmentation of the forest edge and the use of look-up tables for the reflectivity of a single cylinder, a straightforward calculation procedure can be achieved, which allows an implementation in engineering sound propagation models.
A validation of the model showed good agreement with measurements. Nevertheless the measurements indicated a tendency to overestimate the levels at frequencies above 1 kHz. Further measurements should be conducted to shed light on this question and to expand additional aspects such as meteorological influences on forest reflections and the behaviour over hilly terrain where a vertical directivity pattern will become important.

PACS no. 43.20.El, 43.20.Fn, 43.28.Js

1. Introduction

Reflections from forests can have a significant influence on sound exposure, mainly in cases where either the sound source or the receiver is close to the forest edge. In situations where the direct sound is shielded, the reflection from the forest can even become the dominant sound path. Many publications deal with sound propagation through forests or within forested areas [1], [2], [3], [4], [5], [6], [7], [8], [9], [10], [11]. However little research has dealt with the topic of scattered sound at forest edges. Two calculation models have been developed in Switzerland that aim at predicting the A-weighted Max-levels with time weighting FAST for shooting noise. Hofmann [12] divides the forest into small scattering volumes, where each cell is represented by a secondary sound source. The source strength is proportional to the cell volume and the incoming sound intensity, that is attenuated with increasing depth. It has a single free parameter to adjust the secondary source strength. This was determined to achieve a best fit with measurements separately for muzzle blast and sonic boom. The standard model to calculate shooting noise from small arms in Switzerland SL-2000 [13], [14] predicts forest reflections using an empirical formula that has been derived based on ray tracing simulations [15]. The trees were modelled as vertical cylinders. This assumption is in accordance with a study of Embleton [16] who modelled the sound transmission through a forest based on the theory of scattering of plane waves by cylinders. Both models yield reliable results compared to measurements. However their application is restricted to shooting noise and they neither deliver spectral information nor sound exposure level.

Here we present a model for sound reflection, based on the theory of scattering of spherical waves by cylinders, that predicts spectra of reflected sound. The method is derived from scattering theory and numerical computations, but the resulting formulas are simple enough for implementation in engineering models for outdoor noise. The basic concept of the model has already been presented at the Thirteenth international congress on sound and vibration in Vienna 2006 [17]. Since then the calculation method has been extended and validated with measurements.

The present publication starts with the description of the model which is derived from the reflection of a single tree and then extended to the reflection of a row of trees and an entire forest. The complete model is finally compared with measurements and the results are discussed.

Received 23 June 2008, revised 4 September 2008,
accepted 20 October 2008.

2. Model

2.1. Reflection from a single tree

For sound propagation modelling the frequency range of interest typically lies between 63 Hz and 4 kHz. As a consequence of the associated wavelengths ranging from several centimetres up to metres, reflections at small branches, shrubbery and foliage can be neglected. Reflections will occur mainly at the trunks. Therefore it is concluded in accordance with Embleton [16] that the trees can reasonably well be approximated by vertical cylinders. The surface of these cylinders is regarded as smooth and acoustically hard.

From the theory of scattering of spherical waves (see [18], [19], [20]) the following expression for reflectivity ρ of a infinitely long cylinder has been derived by Salomons [17] (reflectivity ρ is defined here as the fraction of acoustic energy that is reflected),

$$\rho_n = \left[\sum_{m=0}^{\infty} \varepsilon_m \cos(m\phi_n)(-i)^m H_m^{(1)}(kr) \frac{J_m'(ka)}{H_m^{(1)\prime}(ka)} \right]^2, \quad (1)$$

where ϕ is the scattering angle, i.e. the angle between incoming and reflected sound, r is the shorter distance from the cylinder to the source or the receiver, $k = \omega/c$ is the wave number defined as the ratio of the angular frequency ω and the sound speed c, a is the radius of the cylinder, and $\varepsilon_0 = 1$, $\varepsilon_m = 2$ for $m \geqq 1$. Further, $H_m^{(1)}$ is the Hankel function of the first kind, $H_m^{(1)\prime}$ its derivative, and J_m' the derivative of the Bessel function J. For numerical calculations, the sum in equation (1) can be truncated at $m = 40$ for all frequencies.

Figure 1 shows three examples of reflectivity ρ given by equation (1) as a function of frequency. In the first graph the reflectivity ρ is depicted for different cylinder diameters. According to Tables I and II, which yield statistical properties for different types of forests, the cylinder diameter has been set to 27.5 cm for the second and third graphs. The second graph shows the influence of distance r and the third graph the dependency on the scattering angle ϕ.

Note: For the current range of application, the Hankel function of the first kind $H_m^{(1)}(kr)$ is in good approximation inversely proportional to the distance r. For an implementation of ρ in an engineering model it is therefore proposed to use look-up tables consisting of third-octave band spectra for specific scattering angles and a reference distance.

2.2. Reflection from an entire forest

Considering Tables I and II it becomes obvious that in a forest trees stand quite far from each other and that the forest as a whole exhibits a very low density. Less than 0.4 percent of the area is actually occupied by trees with only about 5 trees per 100 m^2. The results presented in Figure 1 show that for all frequencies of interest only a small percentage of the energy is reflected at a single tree. Although the number of higher-order reflections is larger than the number of first-order reflections, it can be deduced that higher-order reflections can be neglected for an engineering model as presented here.

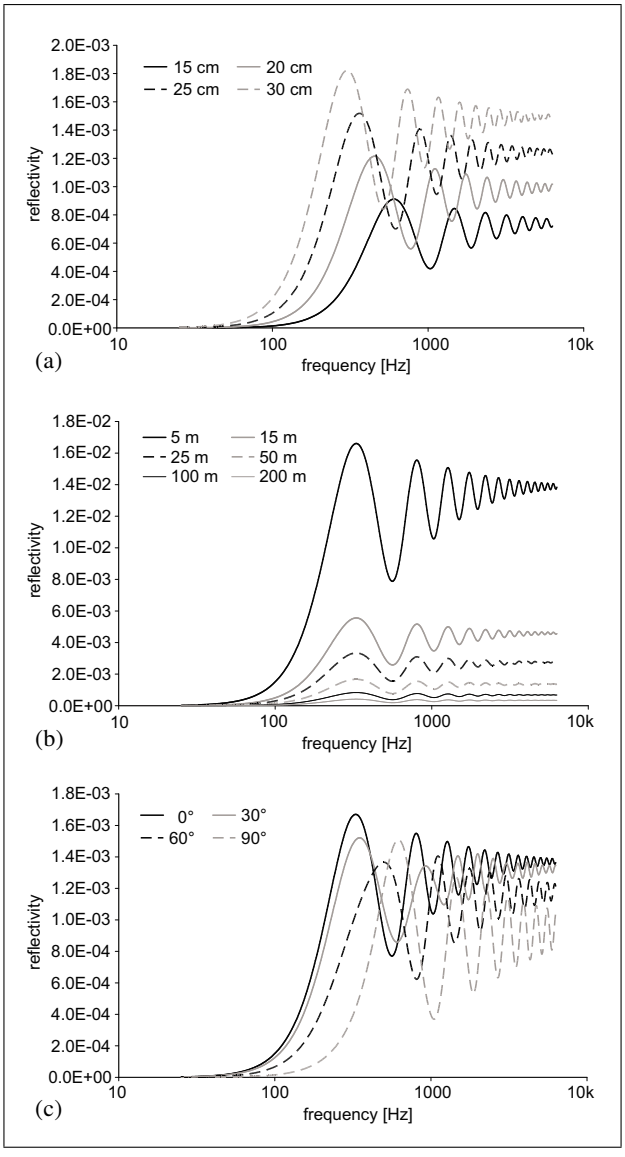

Figure 1. Reflectivity of a cylinder for varying diameters (a), distances (b) and scattering angles (c). When kept constant the scattering angle was set to 0°, the distance to 50 m and the cylinder diameter to 27.5 cm.

In a typical forest the trees are not positioned in a regular grid but show within certain limits an arbitrary distribution. The reflections of numerous trees therefore do not arrive at a receiver in a regular temporal pattern but rather randomly. The summation of the reflected signals of the single cylinders can therefore be carried out incoherently.

As a consequence of the low density, forests are to a large extent transparent for low frequencies. Higher frequencies however are significantly more attenuated. For a forest of 100 m depth the foliage attenuation according to ISO 9613-2 [21] yields 3 dB at 125 Hz, 5 dB at 500 Hz and

Table I. Statistics of the tree population in forests, representative for Switzerland up to 1000 m above sea level [31]. The average takes the frequency of occurrence of the different forest types into account. The diameter as well as the basal plane were measured at a height of 1.3 m. Only trees with diameters of 12 cm or more were counted (for more details see Annex 5.1).

forest type	trees [N/100 m^2]	basal plane [m^2/100 m^2]	average diameter [cm]	average height [m]
>90% softwood	5.38 ±5%	0.386 ±5%	26.8 ±5%	21.8 ±5%
>50% softwood	4.70 ±5%	0.355 ±5%	27.8 ±5%	22.0 ±5%
>50% hardwood	4.48 ±6%	0.308 ±6%	26.5 ±6%	21.0 ±6%
>90% hardwood	4.76 ±5%	0.266 ±4%	23.7 ±5%	18.5 ±5%
average	4.83 ±2%	0.326 ±2%	26.1 ±2%	20.7 ±2%

Table II. Statistics of the tree population in forest edges (first 30 m), representative for Switzerland up to 1000 m above sea level [31]. The average takes the frequency of occurrence of the different forest types into account. The diameter as well as the basal plane were measured at a height of 1.3 m. Only trees with diameters of 12 cm or more were counted (for more details see Annex 5.1).

forest type	trees [N/100 m^2]	basal plane [m^2/100 m^2]	average diameter [cm]	average height [m]
>90% softwood	6.11 ±14%	0.453 ±13%	27.5 ±14%	22.1 ±14%
>50% softwood	5.26 ±10%	0.418 ±10%	28.5 ±11%	22.5 ±11%
>50% hardwood	4.75 ±12%	0.361 ±12%	27.7 ±13%	21.8 ±13%
>90% hardwood	4.50 ±9%	0.314 ±9%	26.4 ±10%	20.2 ±10%
average	5.01 ±5%	0.374 ±5%	27.5 ±6%	21.5 ±6%

8 dB at 2 kHz[1]. This means that half of the sound energy passes the forest at 125 Hz, but only one sixth at 2 kHz, when not taking other attenuating effects into account. Regarding forest reflection it can be concluded that reflections will not only stem from the first rows of trees but also from the depth of the forest and that the penetration depth will show a significant frequency dependency.

Nevertheless it is proposed to model the reflection of an entire forest based only on the reflections of a row of cylinders along the forest edge. The advantage of this simplification to calculate the reflection from a line instead of an area lies in a major reduction of the calculation effort. Also for computational efficiency the row of cylinders is divided into a number of segments (see Figure 2). The energy from segment n is approximated by N_n times the energy from a central cylinder, where N_n is the number of cylinders in the segment and L_n is the sound pressure level reflected from the central cylinder of segment n. Additional reflections from the depth of the forest are accounted for by the definition of the number of cylinders per segment as a function of frequency and geometry (see section 2.5). The sound pressure level of the reflected sound is given by the following incoherent sum over the segments,

$$L = 10 \cdot \log\left(\sum_n N_n \cdot 10^{L_n/10}\right). \qquad (2)$$

The segment width d_{seg} can be chosen arbitrarily and does not necessarily have to be a constant. It is recommended to use segment widths that are smaller than the shortest distance between the forest edge and the source or receiver positions in order to avoid significant influences on calculation results as a consequence of the placement of the particular segments.

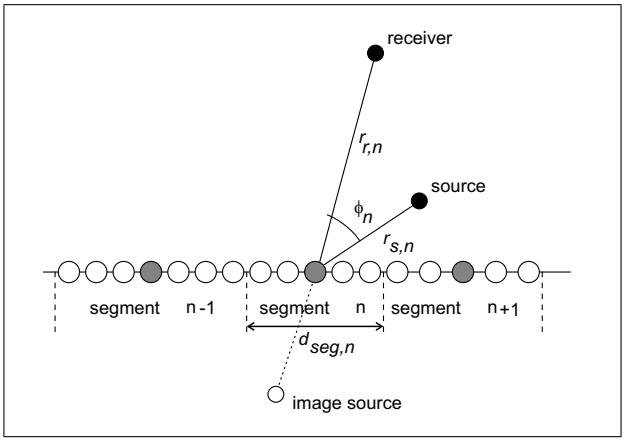

Figure 2. Reflection from a row of cylinders. The row is divided into a number of segments, and each segment is represented by a central cylinder, indicated as a gray circle. An image source is also depicted.

2.3. Propagation calculation

The sound levels of the reflections yielded by the central cylinders of each segment of the forest edge are calculated according to equation (3) where L_W is the sound power level of the source, and the remaining terms are attenuations due to geometrical divergence of the sound field,

[1] The designation foliage attenuation leads one to assume that only the effect of leaves is covered. However according to ISO 9613-2 the foliage attenuation includes all additional attenuating effects for propagation through forested areas.

atmospheric absorption, ground effect and reflection, respectively.

$$L_n = L_W - A_{\mathrm{geo},n} - A_{\mathrm{atm},n} - A_{\mathrm{gr},n} - A_{\mathrm{refl},n}. \qquad (3)$$

Geometrical divergence is calculated with $A_{\mathrm{geo},n} = 10 \cdot \log[4\pi(r_{r,n} + r_{s,n})^2]$ and the atmospheric absorption is defined as $A_{\mathrm{atm},n} = \alpha_{\mathrm{atm}}(r_{r,n} + r_{s,n})$, with absorption coefficient α_{atm}. There exist various methods for calculating the ground attenuation, ranging from engineering models [22], [21], [23], [24] to more advanced models [25], [26]. These methods take into account meteorological influences on the ground attenuation combined with shielding effects. The propagation path for the ground effect calculation is derived by introducing an image source according to Figure 2. It should be borne in mind that not only the source position but also the terrain must be mirrored, including topography and local flow resistance. A peculiarity that has to be taken into account when predicting meteorological effects of reflected sound is that in situations with dominating wind the sound speed profiles vary along the propagation path to the reflector and back. For calculation models that are restricted to a single sound speed profile it is recommended in accordance with [24] to use the meteorological conditions of the longer propagation path, i.e. the path from source to reflector or from reflector to receiver. The reflection attenuation is expressed as

$$A_{\mathrm{refl},n} = -10 \cdot \log(\varepsilon_{\mathrm{ver},n} \cdot \rho_n), \qquad (4)$$

with $\varepsilon_{\mathrm{ver},n}$ the vertical reflection efficiency and ρ_n the reflectivity according to equation (1). Meteorological effects on $A_{\mathrm{refl},n}$ are neglected. The vertical reflection efficiency accounts for the finite height of the trees and is defined by equation (4) applied to a rigid wall, as explained in the next section.

2.4. Vertical reflection efficiency

The vertical reflection efficiency of a forest edge is derived in analogy to the reflection from a wall in a non refracting atmosphere. Equation (5) is based on results of numerical computations of sound reflection from a vertical rigid screen with finite height with the Parabolic Equation (PE) method [26]. The reflection is taken into account by a Kirchhoff approximation: upon reflection the sound pressure at grid points above the screen is set equal to zero. This approach is analogous to the Kirchhoff approach with PE for diffraction into the shadow region behind a screen [27]. The original geometry is shown in Figure 3 together with the equivalent geometry used for the PE computations. The equivalent situation has the advantage that the propagation direction is straight and not reversed at the reflecting screen. The screen height is denoted as H. The source and the receiver are at distances r_s and r_r from the screen, respectively. Based on calculation results of several combinations of frequencies and source distances the engineering approach according to equation (5) has been derived:

$$\varepsilon_{\mathrm{ver}} = \mathrm{Min}\left(1, \frac{\alpha H^2}{\lambda \cdot \mathrm{Min}(r_s, r_r)}\right), \qquad (5)$$

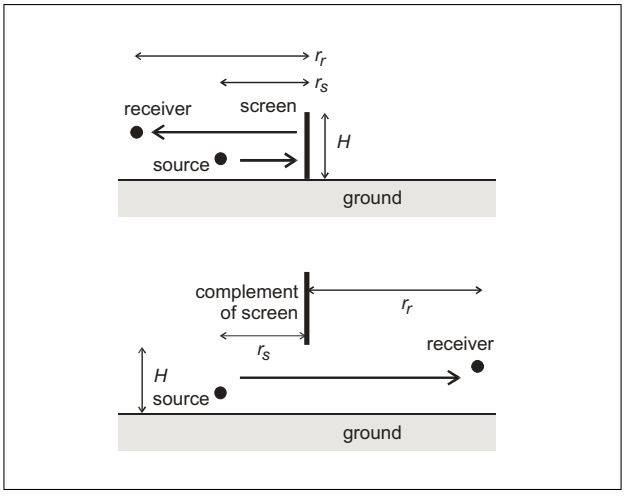

Figure 3. Geometry of a reflection from a screen on a ground surface (top) and its equivalent used for the Kirchhoff approximation (bottom).

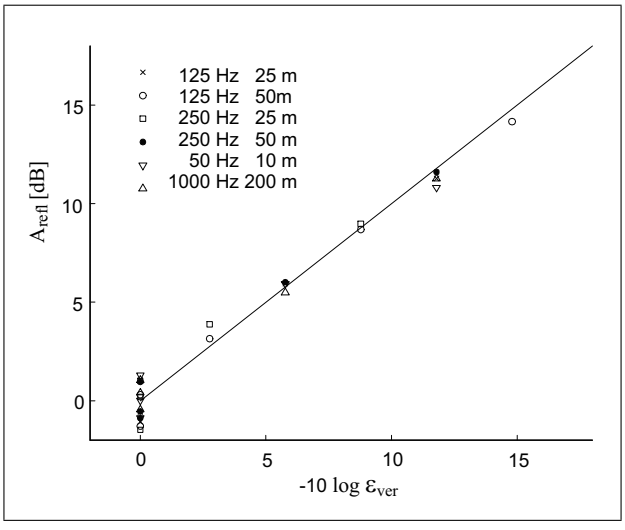

Figure 4. PE results for A_{refl} versus $-10\log(\varepsilon_{\mathrm{ver}})$ with ρ set to 1.

where λ is the wavelength and α is a constant. Figure 4 shows PE results for A_{refl} versus $-10\log(\varepsilon_{\mathrm{ver}})$. The line represents the best fit, and corresponds with $\alpha = 4.5$. The PE results in Figure 4 were determined for a receiver range $r_r = 1000\,\mathrm{m}$, with $A_{\mathrm{gr}} \approx 6\,\mathrm{dB}$ (this value of A_{gr} was verified by a PE computation for $H = \infty$). For forest reflections H is set to 20 m in accordance with Table II.

2.5. Number of trees per segment

The number of trees N per segment in equation (2) takes into account the ratio of the segmentation width d_{seg} and the average distance between trees in the first row of a real forest d_{for}. However in addition it also accounts for reflecting cylinders deeper in the forest. Therefore the number of trees per segment can not solely be calculated from physical properties of the edge of a real forest.

We will now describe how the actual situation with all trees in the forest is approximated by the model situation

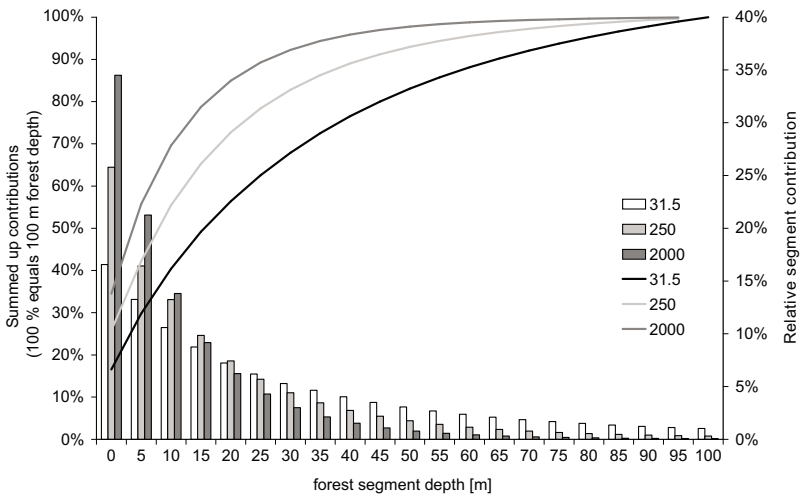

Figure 5. Forest penetration in a situation with a source position at 25 m and a receiver position at 100 m distance from the forest edge, calculated for three octave-bands.

with a single row of trees at the edge of the forest. For that purpose the reflection model is temporarily enhanced in two respects. Instead of a single row of cylinders several rows are taken into account and an additional attenuation term for propagation paths through the forest is introduced. This foliage attenuation per metre according to Table IV is based on ISO 9613-2 [21]. To avoid inconsistencies the attenuations given for propagation distances in the forest from 20 to 200 m are used also for the first 20 m and for greater distances. Dissipation is taken into account according to ISO 9613-1 [28] with average conditions for Switzerland corresponding to a relative humidity of 76% and a temperature of 8°C. Ground effect is neglected here. This corresponds to the assumption that the ground effect is to a first order independent of the position of the reflecting cylinder. Propagation conditions through forested areas as well as the ground conditions sometimes differ significantly from the conditions over open areas exhibiting lower wind speeds and more porous ground (see for example [8]). As it will be shown later, forest reflection stems at least for high frequencies mainly from trees close to the forest edge and therefore sound propagation occurs primarily outside the forest. Thus the above assumption seems admissible.

As foliage attenuation as well as air absorption feature a significant frequency dependency, contributions from the depth of the forest are less important at higher frequencies. Figure 5 shows calculation results for three octave bands for a model forest of 1200 m width and a depth of 100 m, that was represented by a grid of 120 by 20 cylinders. The source was positioned at 25 m from the forest edge and the receiver at 100 m distance with 600 m of forest to both sides. The contributions of rows of cylinders each at 5 m distance are compared to the overall reflection. While the first two rows of cylinders already yield more than 50% of the reflection at 2 kHz, lower frequencies penetrate considerably deeper into the forest. Although trees at 100 m depth still yield a small contribution to the overall reflection at lower frequencies, the reflection of a 100 m deep forest can be taken as representative for forests with greater depth as well.

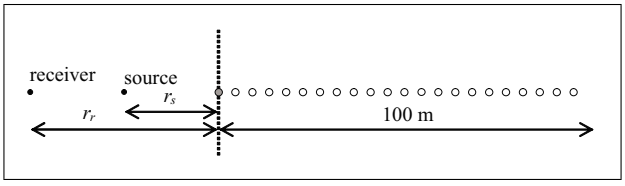

Figure 6. Geometry with source, receiver and all reflecting cylinders perpendicular to an imaginary forest edge (indicated with a dotted line). The situation shows a receiver position at 50 m and a source position at 25 m from the forest edge.

Apart from this frequency dependency the number of representative cylinders in the first row also depends on geometry. The closer the source and / or receiver are to the forest edge the greater will be the change in the geometrical divergence A_{geo} and in the reflection attenuation A_{refl} from cylinders in the first row relative to adjacent ones deeper in the forest. Therefore contributions from the depth of the forest become less important the closer the source and the receiver are to the edge of the forest; consequently the number of representative cylinders in the first row is reduced as well.

In order to derive a relation between the reflection of an entire forest and the contribution of the first row of cylinders, a set of 20 source-receiver-combinations was calculated for a situation with source and receiver as well as all the reflecting cylinders in a line (see Figure 6). This corresponds to a situation with source and receiver in a line perpendicular to the forest edge where only the segment at shortest distance is taken into account. Source positions were set at distances of 7.5, 12.5, 25, 150 and 500 m and receiver positions at 50, 100, 200 and 400 m. 22 reflecting cylinders were set with a constant spacing of 4.5 m, resulting in a forest depth of approximately 100 m. A separation distance of 4.5 m was chosen in order to represent the average forest density according to Table II for a situation

with an equidistant grid of trees. Model calculations were performed for octave bands from 31.5 Hz to 4 kHz.

In the data analysis the reflected contributions of the two model situations, one with a single cylinder and one with a row of cylinders, were compared. It was found that the ratio between the reflection contributions of the two cases exhibits a similar dependency on the logarithm of the wavelength λ for all source-receiver-combinations. Therefore the dependency on frequency and geometry can be derived separately.

The influence of geometry was determined based on a mathematical approach for hyper-areas of the third order by introducing a function u with two free parameters (see equation 6): To reproduce the influence of distance on geometrical attenuation the overall propagation distance squared was introduced and for the distance dependency of the reflectivity ρ the minimum of r_s and r_r was used.

$$u[x, y] = g + h \cdot f_x + i \cdot f_y + j \cdot f_x f_y + k \cdot f_x^2 f_y + l \cdot f_x f_y^2 + m \cdot f_x^2 f_y^2, \quad (6)$$

with $x = \mathrm{Min}(r_r, r_s)$, $y = (r_r + r_s)^2$, $x_{\mathrm{Min}} = 7.5$, $x_{\mathrm{Max}} = 400$, $y_{\mathrm{Min}} = (7.5 + 50)^2$, $y_{\mathrm{Max}} = (500 + 400)^2$, $f_x = \ln(x/x_{\mathrm{Min}})/\ln(x_{\mathrm{Min}}/x_{\mathrm{Max}})$, $f_x = \ln(y/y_{\mathrm{Min}})/\ln(y_{\mathrm{Min}}/y_{\mathrm{Max}})$.

The free parameters were optimized to yield a least-square-fit resulting in the following parameters: $g = 0.484$, $h = -0.387$, $i = -0.203$, $j = -0.713$, $k = 1.313$, $l = 0.814$, $m = -1.171$.

Equation (7) yields the number of trees per segment N with d_{for} set to 4.5 m as a default value. Parameter v accounts for the frequency dependency and was determined as -0.03. N increases with increasing wavelength and propagation distance. With the second criterion in equation (7) it is guaranteed that the number of trees does not exceed the case of a closed wall, i.e. a situation with no space between cylinders. In agreement with equation (1) a is the cylinder radius.

$$N = \mathrm{Min}\left[\frac{d_{\mathrm{seg},n}}{d_{\mathrm{for}}}\frac{1}{u[x, y] + v\ln(\lambda)}, \frac{d_{\mathrm{seg},n}}{2a}\right]. \quad (7)$$

With this approach the underlying calculations could be reproduced with a standard deviation of less than 1 % in all octave bands.

Equations (6) and (7) were derived for the segment having the shortest distance to source and receiver. In order to be sure that the resulting approach is also valid for entire forests, the set of 20 source-receiver-combinations was recalculated for a forest with a length of 1 kilometre and a depth of 100 m. As an equal spacing of 4.5 m was used parallel and perpendicular to the forest edge the model forest consisted of 222 x 22 cylinders. The resulting octave-band spectra of the reflected sound exposure level were compared with calculations of only the first row of cylinders that additionally used the correction for the number of cylinders according to equations (6) and (7). Again the agreement was good with a mean error of -0.3 dB, i.e. a slight overestimation in the case with only one row of cylinders, for all 20 situations and octave-bands. The standard deviation was 0.5 dB.

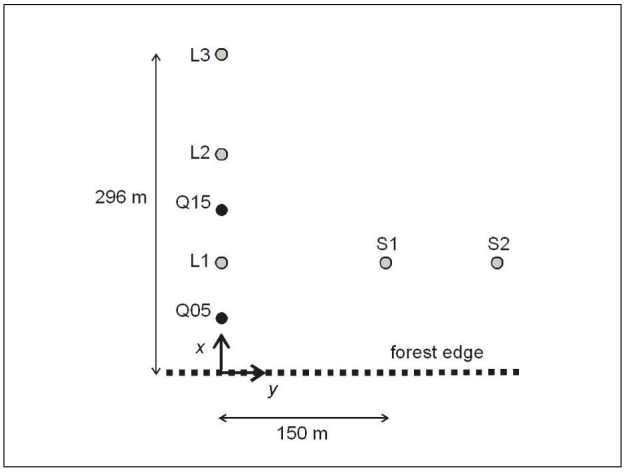

Figure 7. Measurement situation.

Table III. Measurement geometry. (Note: The centre of the coordinate system is placed at the edge of the forest with at least 250 m of forest to each side. X denotes the distance to the forest edge, Y denotes distances parallel to it.)

Receiver	X	Y	Source	X	Y
L1	97 m	0 m	Q05	47 m	0 m
L2	197 m	0 m	Q15	147 m	0 m
L3	296 m	0 m			
S1	100 m	150 m			
S2	100 m	250 m			

3. Comparison with measurements

In order to validate the calculation model, a series of measurements was carried out. The measurement site was a mixed forest with more than 50% hardwood close to Thun in Switzerland. The forest had little shrubbery and average tree heights of 20 m or more. The measurement site was on flat terrain over grassy ground with a straight forest edge of 650 m length and a forest depth between 80 and 120 m. Figure 7 shows the experimental setup, with source positions Q05 and Q15, and microphone positions L1, L2, L3, S1 and S2. The forest edge is located at the horizontal line x = 0. In Table III the coordinates of the source and microphone positions are given. The microphones were placed at a height of 4 m above terrain. The sound source consisted of 50 g charges of explosive material (Plastit), which were ignited on a steel plate on the ground. Table V gives the idealized emission spectrum. According to [29] the effective source height for a point source was set to 0.7 m above ground.

Measurements were performed in November 2007 between 20:00 and 22:00 with calm conditions and a clear sky. These measurement conditions were chosen to guarantee favorable propagation conditions for direct as well as reflected sound. As meteorological parameters temperature, humidity and wind were recorded. Temperature was measured at 1, 3 and 10 m height. The wind vector was captured with an ultrasonic anemometer at height 3 m. The

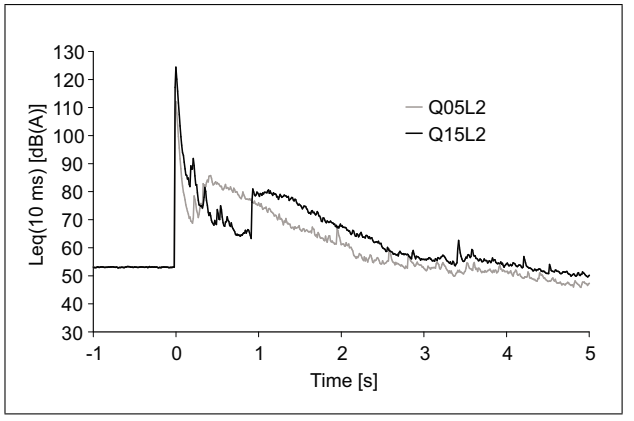

Figure 8. A-weighted level vs. time curves with 10 ms resolution for microphone position L2 and both source positions. The curves show an average over 10 single events. Reflected sound has been analysed after 0.3 s for source Q05 and after 0.9 s for source Q15.

temperature at height 10 m decreased during the measurements from 3.3 to 2.4 °C and was generally about 2 °C higher than at height 1 m. The wind direction was approximately parallel to the forest edge with an average wind speed of 1.2 m/s. These conditions imply that the atmosphere showed a stable stratification, featuring the desired propagation conditions. The relative humidity measured at 1 m height was about 95%.

At each source position 10 explosions were executed. As an example Figure 8 shows level vs. time diagrams for both source positions at receiver L2. For direct and reflected sound sound exposure spectra were derived in octave bands from 63 Hz to 2 kHz and averaged over the 10 measured single events.

The situation was reproduced by calculations according to the model presented in section 2. As a consequence of the forest type d_{for} was set to 4.75 m. The segmentation width d_{seg} was kept at 4.5 m. In order to take the actual meteorological conditions into account the ground effect was calculated with a Parabolic-Equation-Model [26] for receiver positions L1, L2 and L3 that incorporated averaged sound speed profiles derived from measured temperature and wind profiles. A ground impedance typical for natural soil or grassland was assumed, using the Delaney and Bazley [30] impedance model with a flow resistivity of 200 kPa s/m^2. Calculations were not performed for each segment separately but for a situation with a rigid wall along the forest edge. Figure 9 shows the resulting ground attenuations for direct and reflected sound.

For the given source and receiver combinations equation (7) yields values for the number of trees N per segment that range from 3.1 to 12.0 depending on frequency and the segment under consideration. Hence the limiting criterion of 16.4 trees per segment is not reached. The number of trees for the segments at the largest distance relative to the shortest distance is larger by a factor 1.8. Thereby the ratio between the number of trees per segment at octave-bands of 31.5 Hz and 4 kHz ranges from 1.9 to 2.8.

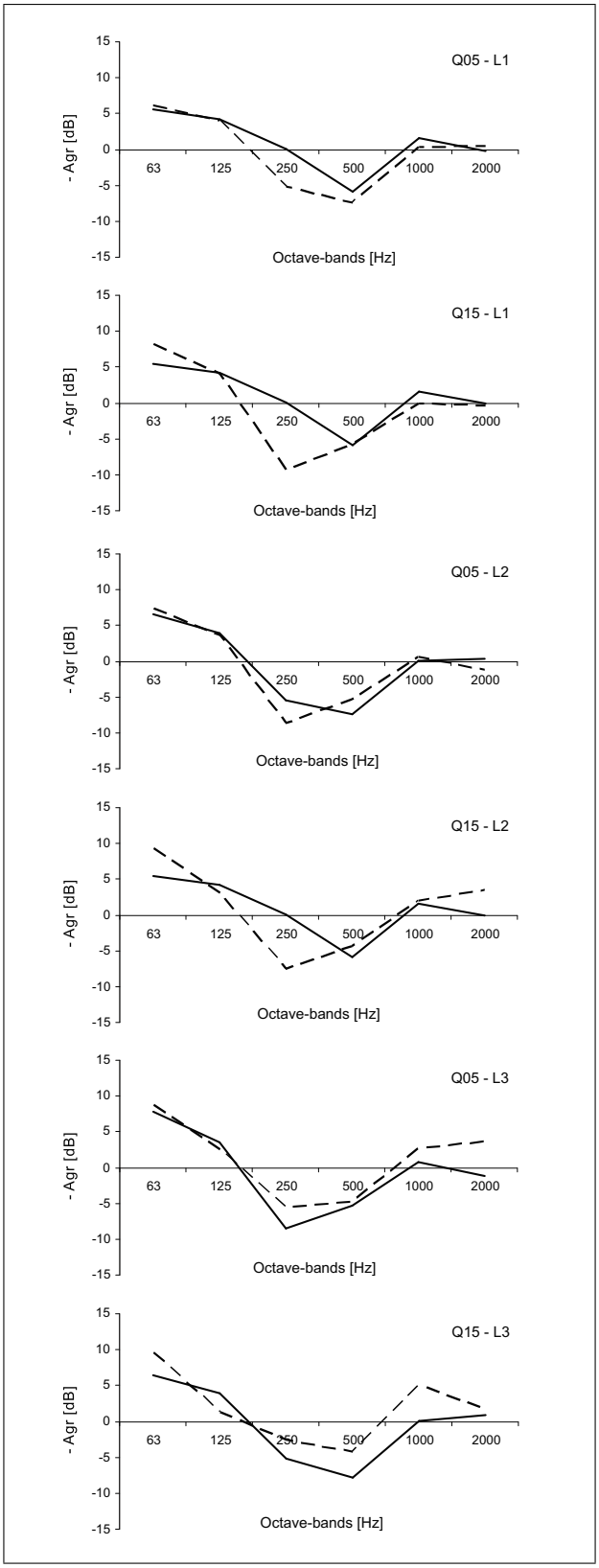

Figure 9. Calculated ground attenuation for direct sound and a reflection on a rigid wall (solid and broken lines).

Figure 10 shows a comparison of the measured and calculated spectra of direct and reflected sound. The measured direct sound yielded between 16 and 31 dB(A)

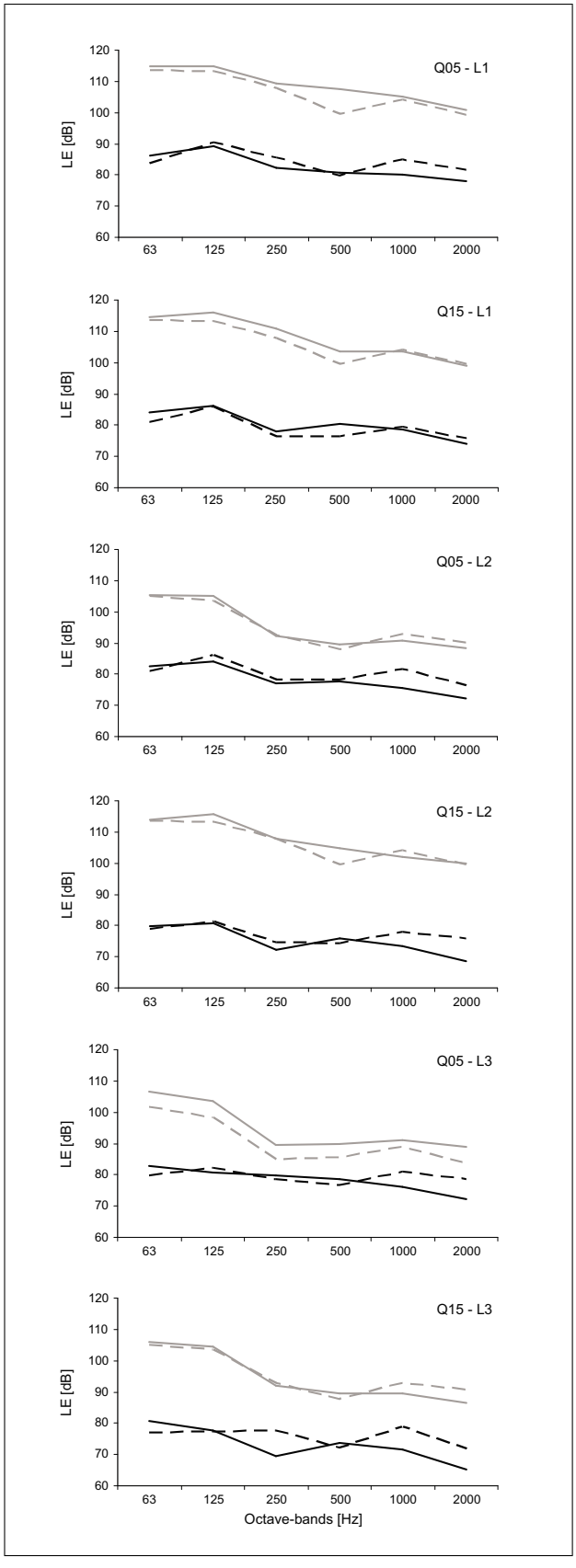

Figure 10. Measured and calculated octave band spectra (solid and broken lines) of the sound exposure level of direct and reflected sound (grey and black lines).

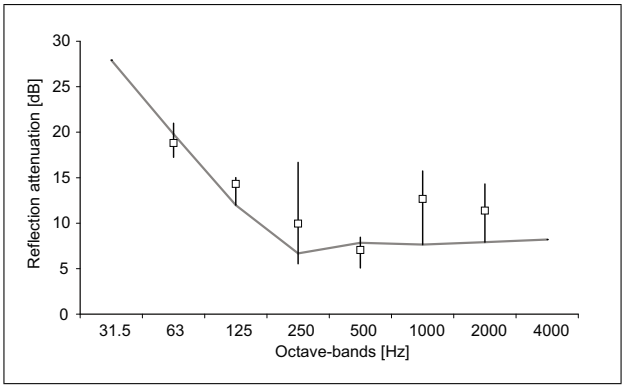

Figure 11. Measured reflection attenuations (squares with vertical lines indicating average, maximum and minimum values) in comparison with a calculated reflection attenuation for a representative geometry (source at 100 m and receiver at 200 m from the forest edge, forest segment at 119 m away from the shortest distance, representing the average angle of incidence).

higher level than the reflection. Generally the direct sound could be reproduced with good accuracy although the typical ground effect dip sometimes was not so prominent in the measured spectra as predicted. The average deviation between measurement and calculation of the direct sound was 0.7 dB(A), i.e. a slight underestimation of the measured values.

Generally the spectral course of the reflected sound also shows a good agreement between measurement and calculation. While at lower frequencies the measured values are reproduced very well, there is a tendency for overestimation between 1 and 2 kHz. This results in an averaged A-weighted level which is 3.5 dB higher than measured.

In order to obtain an integral comparison of the measurements with calculations Figure 11 shows an analysis of measured versus calculated reflection attenuations A_{refl} for a situation with a representative geometry. The measured reflectivities were derived as a difference between the measured propagation attenuation and the propagation attenuations calculated for the reflection on a wall. The calculated reflectivity ρ was derived as an average over all cylinders along the forest edge. The number of trees N per segment amounts to 10.0 at 31.5 Hz and 4.1 at 4 kHz, equalling effective cylinder spacings of 0.5 m and 1.2 m. As can be seen the measured frequency dependency is generally well reproduced by the calculation. Although the calculated values deviate in some octave bands significantly from the measured averages, they are still within the range of the measured values. Based on a data set of only 6 measured spectra it is hardly possible to decide whether the assessed deviations are systematic or not.

4. Conclusions

The presented calculation procedure is based on an analytical solution for the reflection from a cylinder. Thanks to several model assumptions a rapid calculation and thus an implementation in engineering sound propagation models

is feasible. The use of look-up tables for the reflectivity, the reduction of an entire forest to a line of reflectors, the variable segmentation and the incoherent superposition of signals allow a significant reduction of the calculation effort.

Despite these simplifications first comparisons with measurements indicate a good accuracy of the model. The predicted frequency dependency of forest reflection resulting from the combination of a single cylinder reflection with a variable effective spacing between cylinders as a function of frequency and geometry appears to be confirmed. Nevertheless the measurements indicate a tendency to overestimate the levels at frequencies above 1 kHz. Possible explanations for this behaviour might be found in deviations in the propagation calculation, the characteristic of the forest at the measurement site or the assumed foliage attenuation that was used to derive the effective spacing between cylinders. However the existing data base is not large enough to investigate this aspect in more detail. Until the model is compared to additional measurements these deviations have to be assigned to the uncertainty of the model.

The transformation from an area of reflecting cylinders to a line was performed for a model forest of 100 m depth. For the frequency range of interest this forest depth is sufficient to be representative for wider forests as well. In contrast to a very small forest the reflection will comply with the reflection of a single line of trees, which is attained when the number of cylinders N per segment according to equation (7) approximates the physical density of trees. Accordingly a feasible approach would be to weight the number of cylinders N per segment with the actual forest depth.

Apart from additional measurements to validate the model further investigations would also be recommended to assess meteorological influences on the reflected sound and to derive the vertical directivity of forest reflections. The model has so far only been tested based on measurements on level ground with source, reflector and receiver at comparable heights. Situations with sound sources and receiver positions with clearly deviating heights, resulting in significant vertical radiation angles for the forest reflection, are typical in valleys and yield considerable echos. Based on the conception of cylinders one might expect a vertical directivity pattern that clearly deviates from the horizontal case. Therefore an expansion of the model towards a three dimensional description of the reflectivity might be appropriate.

5. Annex

5.1. Forest characterization

As a basis for the modelling it is necessary to characterize the tree population in forests. Statistics of the Swiss Federal Institute for Forest, Snow and Landscape Research provide information on the number of trees per area, their total area, the average and the standard deviation of their diameter and their average height. The data is generally separated for four forest types and two heights, forests higher and lower than 1000 m above sea level. In Table I on page 3 averaged data for forests below 1000 m above sea level is combined.

Regarding the topic of this publication additional evaluations have been carried out for the tree population of the forest edge [31]. Table II shows the data available for the first 30 m of depth for forests below 1000 m above sea level. In comparison with Table I it can be deduced that, most likely as a consequence of better insolation, the forest density is generally higher at the forest edge, regardless the forest type. Above 1000 m sea level the forest density as well as the size of the trees is reduced, both in the depth of the forest and on the edges.

It is proposed to use the average data of Table II as default values for the forest reflection model. It has to be borne in mind though that these parameters, especially the number of trees and consequently also the basal plane, can vary significantly between different forest types. A forest consisting of more than 90 % coniferous trees shows a more than 20 % higher density than in the average case, resulting in an increase of the forest reflection of 0.8 dB. Similar differences in level result from changes of the average tree diameter.

Table IV. Foliage attenuation per metre propagation through forest (adopted from [21]).

31.5 Hz	63 Hz	125 Hz	250 Hz
0.01	0.02	0.03	0.04
500 Hz	1000 Hz	2000 Hz	4000 Hz
0.05	0.06	0.08	0.09

Table V. Weber spectrum (see [32]) of an explosion of 50 g Plastit in octave-bands at a reference distance of 1 m.

31.5 Hz	63 Hz	125 Hz	250 Hz
138.1	142.1	143.2	141.9
500 Hz	1000 Hz	2000 Hz	4000 Hz
139.4	136.6	133.6	130.7

5.2. Foliage attenuation

Table IV gives values of foliage attenuation per metre propagation through a forest.

5.3. Explosion emission data

Table V shows the emission data at a reference distance of 1 m that was used to reproduce the measurements according to section 3 by calculation.

Acknowledgment

This work was supported by the Defence Procurement Agency of Switzerland (armasuisse), the Federal Office for the Environment of Switzerland (bafu) and the Dutch Ministry of Defence (DRMV). A special thank goes to A.

Zingg and U. Ulmer from the Swiss Federal Institute for Forest, Snow and Landscape Research (WLS) which provided the information on forest properties.

References

[1] D. E. Aylor: Sound transmission through vegetation in relation to leaf area density, leaf width and breadth of canopy. Journal of the Acoustical Society of America **51** (1972) 411–414.

[2] D. E. Aylor: Comments on foliage as a low-pass filter: Experiments with model forests in an anechoic chamber. Journal of the Acoustical Society of America **70** (1981) 891.

[3] W. H. T. Huisman, M. J. M. Martens: A ray tracing model of forest acoustics. Proceedings of the Workshop on Sound propagation in forested areas and Shelterbelts, 1986.

[4] W. H. T. Huisman, K. Attenborough: Reverberation and attenuation in a pine forest. Journal of the Acoustical Society of America **90** (2664-2677) 1991.

[5] M. J. M. Martens: Foliage as a low-pass filter: Experiments with model forests in an anechoic chamber. Journal of the Acoustical Society of America **67** (1980) 66–72.

[6] M. J. M. Martens, A. Michelsen: Absorption of acoustic energy by plant leaves. Journal of the Acoustical Society of America **69** (1981) 303–306.

[7] M. A. Price, K. Attenborough, N. W. Heap: Sound attenuation through trees: Measurements and models. Journal of the Acoustical Society of America **84** (1988) 1836–1844.

[8] M. Ringheim: Attenuation of sound through vegetation: Some results from a literature survey. Proceedings of the workshop on sound propagation in forested areas and shelterbelts, 1986.

[9] J. C. Rogers, P. Chen: An acoustic scattering model for forests. Journal of the Acoustical Society of America **90** (1991) 2368ff.

[10] M. Swearingen et al.: Survey of research on sound propagation in forests. Proc. 8th Symp. on Long-Range Sound Prop., Pennsylvania State University, 1998, 131–138.

[11] A. I. Tarrero, M. A. Martin, J. Gonzalez, M. Machimbarrena, F. Jacobsen: Sound propagation in forests: A comparison of experimental results and values predicted by the Nord 2000 model. Applied Acoustics **69** (2008) 662–671.

[12] R. Hofmann: Streuung von Schiesslaerm an Waldpartien. Jahrestagung der Deutschen akustischen Gesellschaft, 1988, 355–358.

[13] Bundesamt fuer Umwelt, Wald und Landschaft (BUWAL): Schiesslaerm-Modell SL-90, Erweiterung. Bundesamt fuer Umwelt, Wald und Landschaft, Dokumentationsdienst, 1996.

[14] Bundesamt fuer Umwelt, Wald und Landschaft (BUWAL): PC-Programm SL-2000, Version 1.0. Bundesamt fuer Umwelt, Wald und Landschaft, Dokumentationsdienst, 1997.

[15] A. Rosenheck, R. Keller: Recent advances in the control and prediction of rifle noise. Internoise 96, Proceedings Internoise '96, Liverpool, 1996.

[16] T. F. W. Embleton: Scattering by an array of cylinders as a function of surface impedance. J. Acoust. Soc. Am. **40** (1966) 667–670.

[17] E. M. Salomons: A model for calculating specular and diffuse reflections in outdoor sound propagation. The Thirteenth International Congress on Sound an Vibration, ICSV13, Vienna, Austria, July 2-6, 2006.

[18] J. J. Bowman, T. B. A. Senior, P. L. E. Uslenghi: Electromagnetic and acoustic scattering. North-Holland, Amsterdam, 1969. 92-128.

[19] P. M. Morse, K. U. Ingard: Theoretical acoustics. McGraw-Hill, New York, 1968.

[20] J. R. Wait: Electromagnetic radiation from cylindrical structures. Pergamon, London, 1959. 1-28.

[21] International Standard ISO 9613-2: Acoustics - Attenuation of sound during propagation outdoors. Part 2: General method of calculation. 1996.

[22] J. Hofmann, K. Heutschi: An engineering model for sound pressure in shadow zones based on numerical simulations. Acta Acustica united with Acustica **91** (2005) 661–670.

[23] B. Plovsing, J. Kragh: Nord2000: Comprehensive outdoor sound propagation model. Delta Acoustics & Vibration Report AV 1849/00, 2006.

[24] D. van Maercke, J. Defrance: Development of an analytical model for outdoor sound propagation within the Harmonoise project. Acta Acustica united with Acustica **93** (2007) 201–212.

[25] R. Blumrich et al.: A linearized eulerian sound propagation model for studies of complex meteorological effects. Journal of the Acoustical Society of America **112** (2002) 446–455.

[26] M. Salomons: Computational atmospheric acoustics. Kluwer Academic Publishers, Dordrecht, 2001.

[27] E. M. Salomons: Diffraction by a screen in downwind sound propagation: a parabolic-equation approach. J. Acoust. Soc. Am. **95** (1994) 3109–3117.

[28] International Standard ISO 9613-1: Acoustics - Attenuation of sound during propagation outdoors. Part 1: Calculation of the absorption of sound by the atmosphere. 1993.

[29] J. M. Wunderli: Modelling the source strength of explosions under consideration of the ground influence. Acta Acustica united with Acustica **90** (2004) 690–701.

[30] M. E. Delany, E. N. Bazley: Acoustical properties of fibrous absorbent materials. Applied Acoustics **3** (1970) 105–116.

[31] U. Ulmer: Schweizerisches Landesforstinventar LFI. Spezialauswertung der Erhebung 1993–95 vom 24. Februar 2003. Swiss Federal Institute for Forest, Snow and Landscape, 2003.

[32] ISO/TS 13474: Acoustics - Impulse sound propagation for environmental noise assessment. 2003.